Localization and cluster formation in light nuclei

Dario Vretenar

Localization and clustering in nucleonic matter

B. Mottelson - quantality parameter: $$\Lambda_{\rm Mot} \hat{=} \frac{\hbar^2}{m\bar{r}^2|V_0|}.$$ ratio of the zero-point kinetic energy of the confined particle to its potential energy.

The transition between a solid phase (small kinetic energy compared to the potential at equilibrium) and a liquid (large kinetic energy in comparison to the depth of the potential) occurs for $\Lambda_{\rm Mot} \cong 0.1$.

Nuclear matter: $\bar{r} \sim 1$ fm, $|V_0| \sim 100$ MeV → $\Lambda_{\rm Mot} \sim 0.4$ quantum liquid phase.

Liquid–cluster transition in finite nuclei

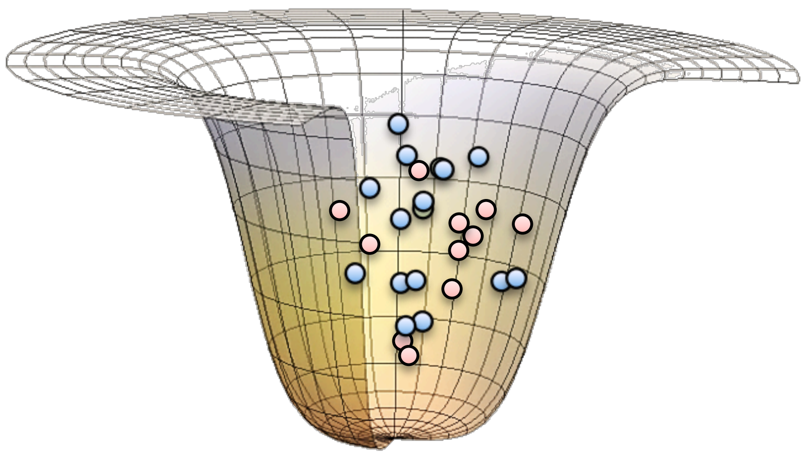

…dimensionless localisation parameter: $$\alpha_{\rm loc} \hat{=} \frac{\Delta r}{\bar{r}},$$

$\bar{r}$ is the average inter-nucleon distance, and Δr the spatial dispersion of the wave function:

$$\Delta r = \sqrt{\langle r^2 \rangle - \langle r \rangle^2}.$$

J. Phys. G: Nucl. Part. Phys. **44** (2017) 103001

When the confining nuclear potential is approximated by a three-dimensional isotropic harmonic oscillator:

$$\alpha_{\text{loc}} \simeq \frac{b}{r_0} = \frac{\sqrt{\hbar R}}{r_0(2mV_0)^{1/4}}$$

b is the oscillator length and r_0 = 1.25 fm. Using the liquid-drop parameterization for the radius R = $r_0 A^{1/3}$

$$\alpha_{\text{loc}} = \frac{\sqrt{\hbar}A^{1/6}}{(2mV_0 r_0^2)^{1/4}} \simeq 0.67A^{1/6}$$

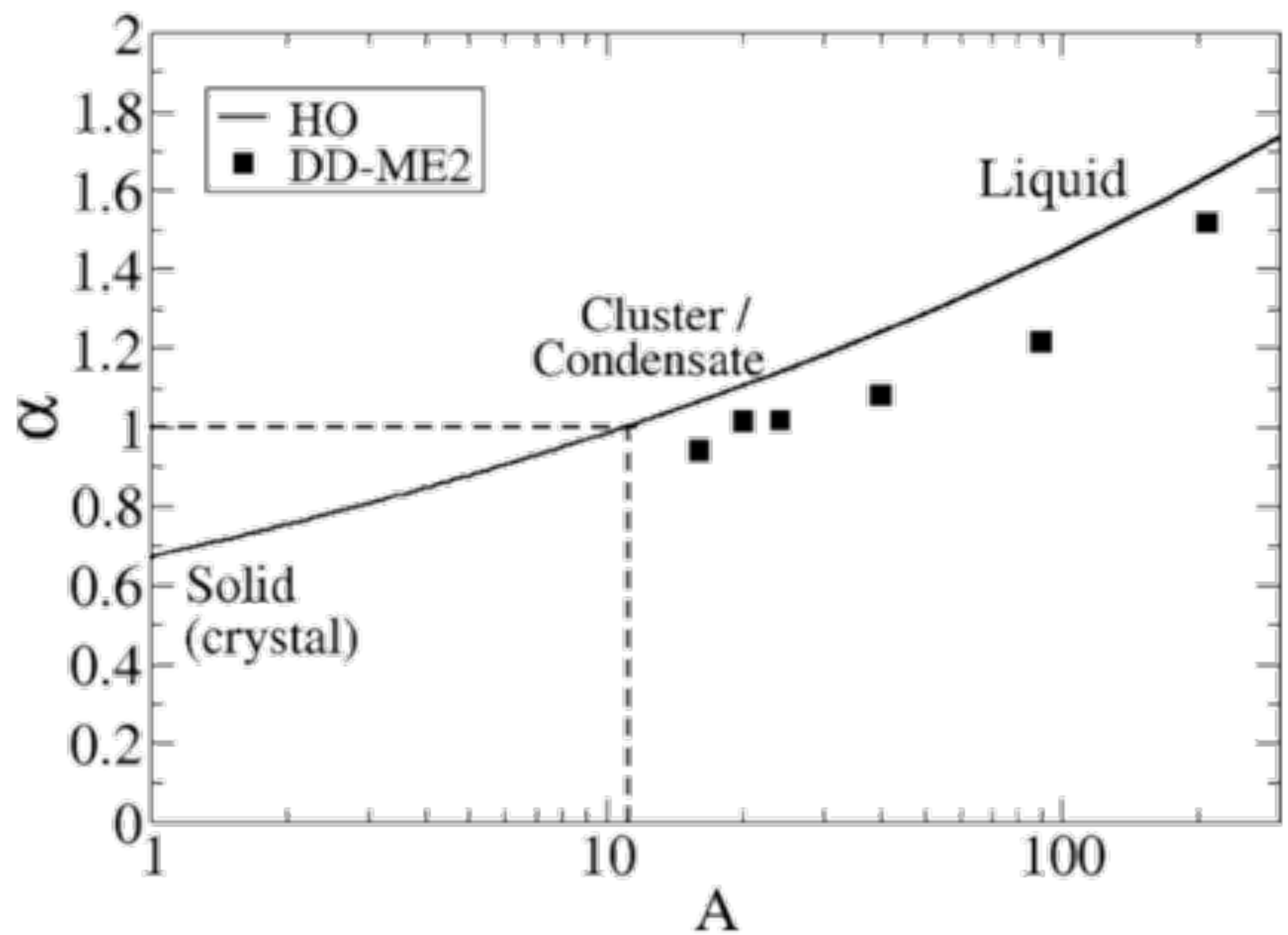

The transition from coexisting cluster and mean-field states to a Fermi liquid state occurs for A ~ 20 - 30. In heavier systems $\alpha_{loc} > 1$ → heavy nuclei consist of largely delocalized nucleons characterized by a large mean free path.

Clusters in light α-conjugate nuclei

Important role of nuclear shape deformation: removes the degeneracy of single- nucleon levels associated with spherical symmetry.

The saturation of inter-nucleon forces, effective when both spin and isospin are coupled to zero, produces a particularly strong binding of the α-cluster and a central density that is by almost a third larger than central densities in most nuclei.

Self-consistent mean-field intrinsic reflection-asymmetric and reflection-symmetric axial densities of ^{20}Ne.

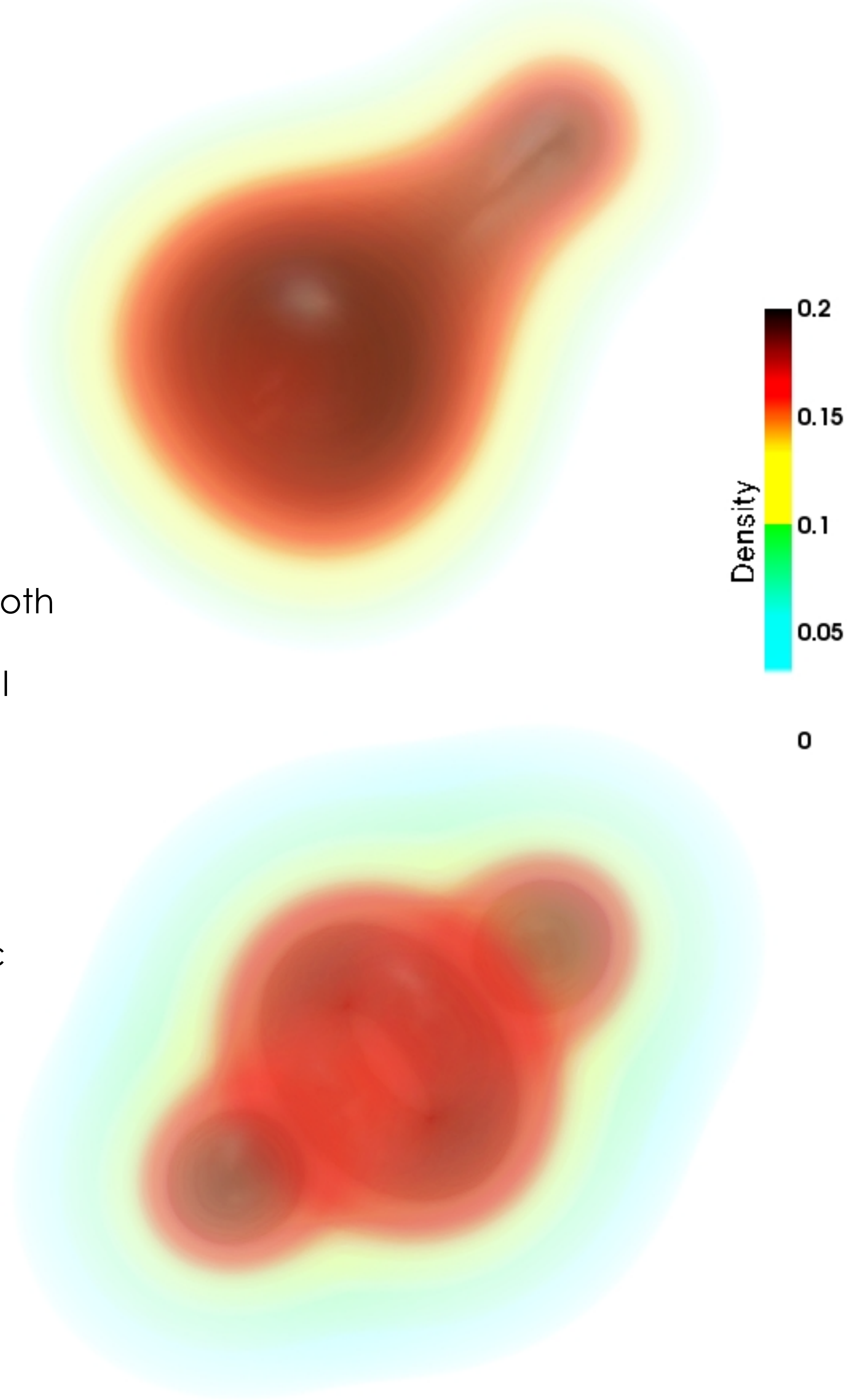

J. Phys. G: Nucl. Part. Phys. **44** (2017) 103001

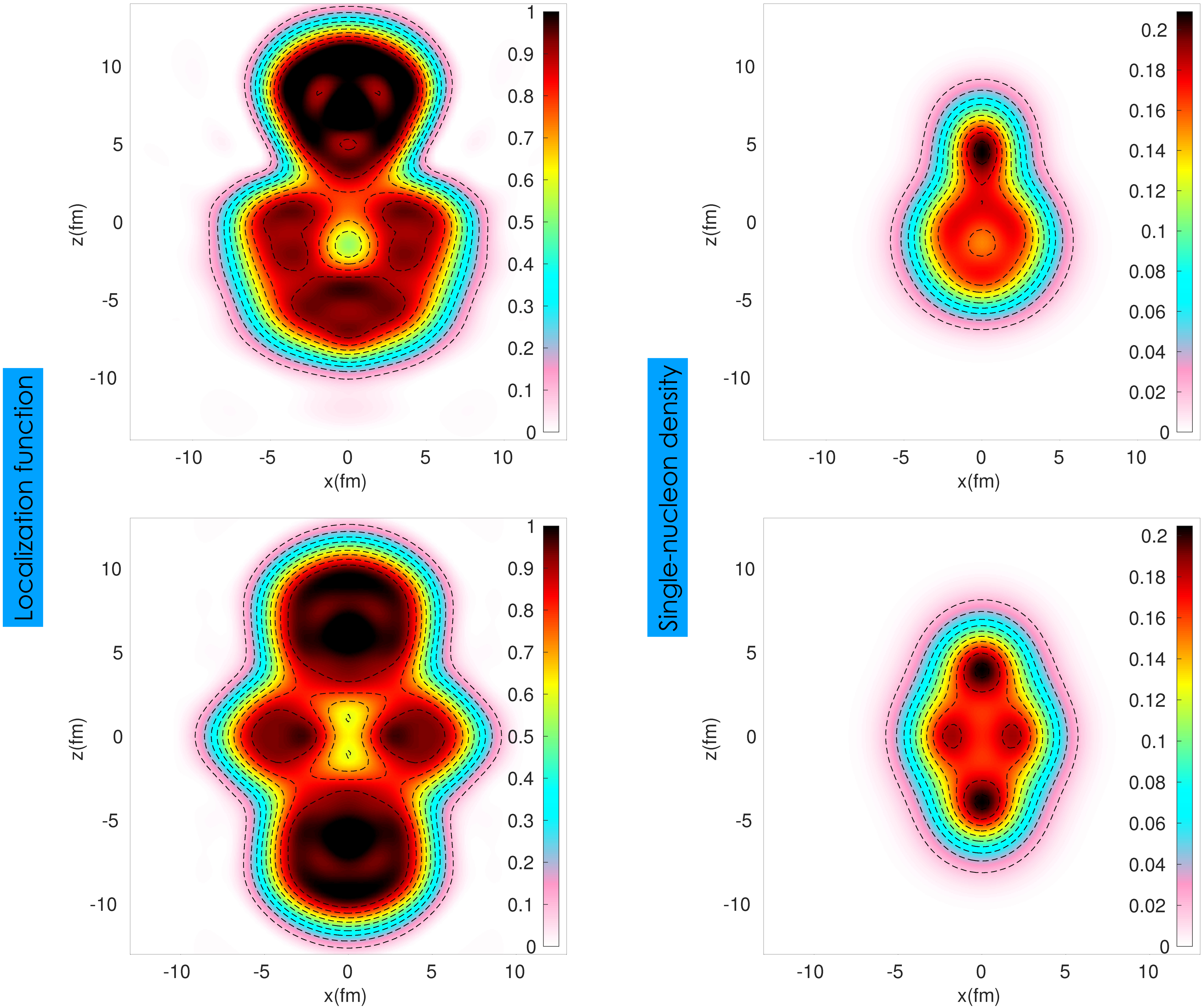

Localization function
Single-nucleon density
z(fm)
x(fm)
-10
-5
0
5
10
0
0.1
0.2
0.3
0.4
0.5
0.6
0.7
0.8
0.9
1
0
0.02
0.04
0.06
0.08
0.1
0.12
0.14
0.16
0.18
0.2

Dilute nuclear matter in excited configurations => the formation of clusters locally enhances the nucleonic density toward its saturation value, increasing the binding of the system.

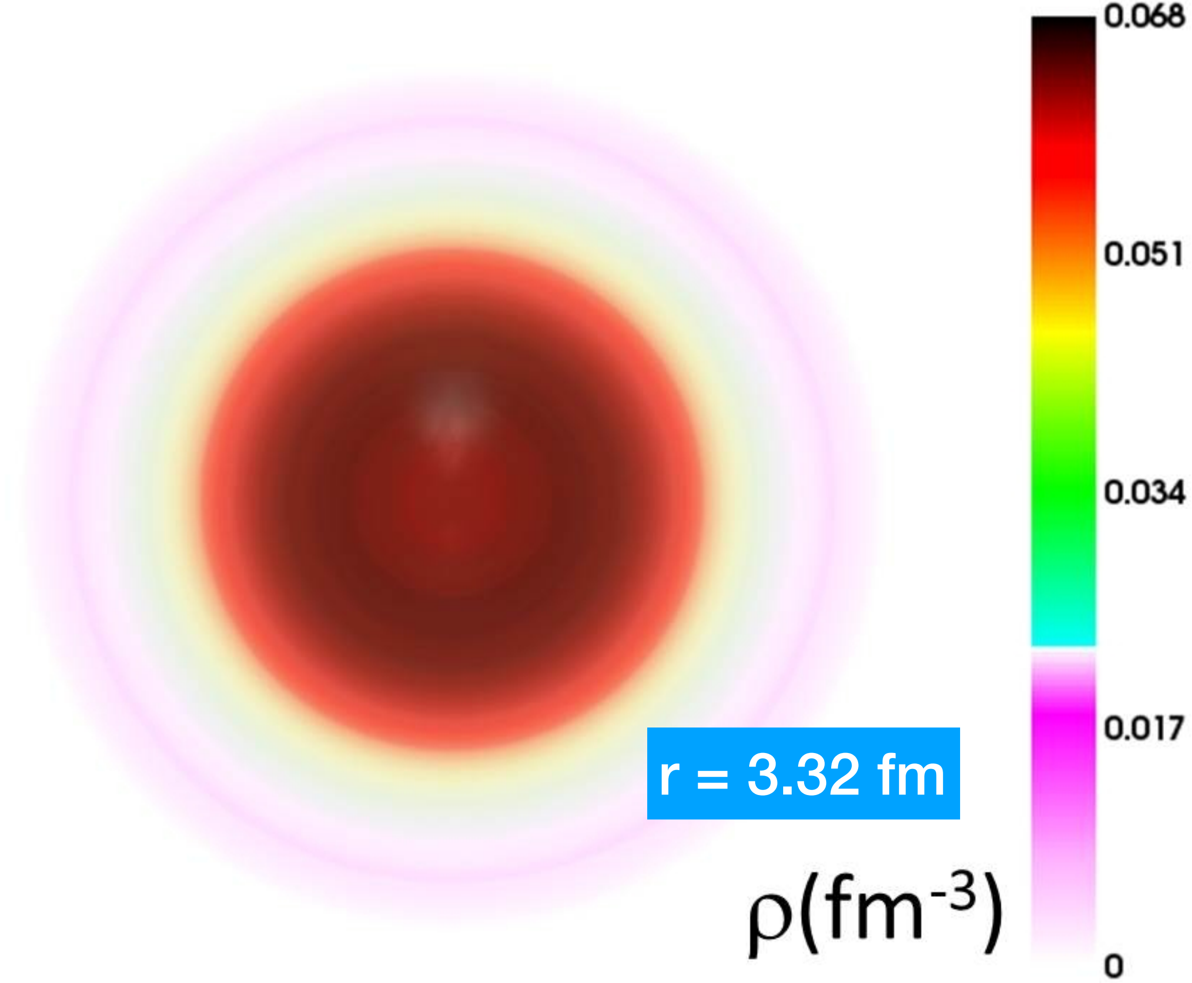

Constrained self-consistent mean-field densities of ^{16}O.

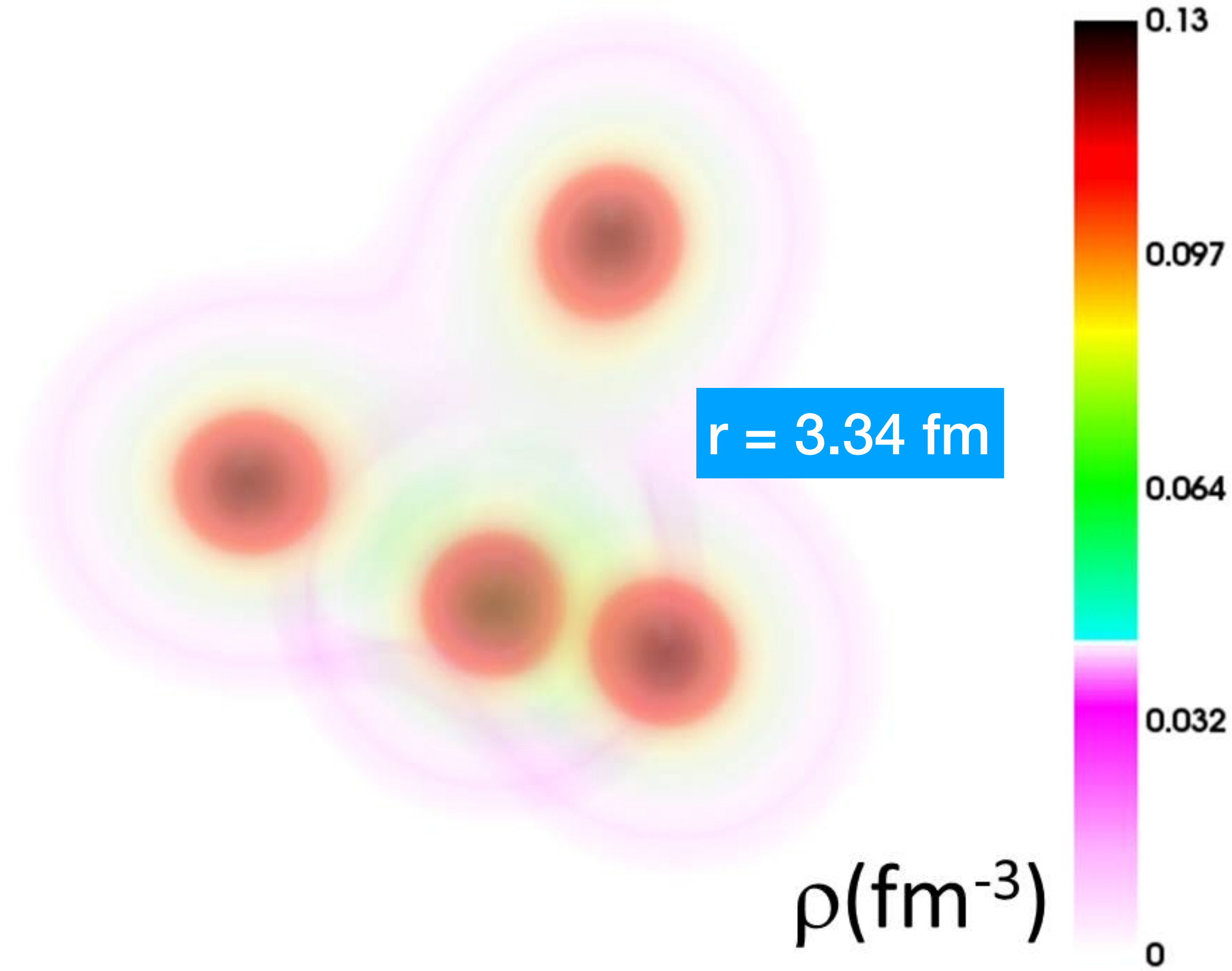

J. Phys. G: Nucl. Part. Phys. **44** (2017) 103001

Constrained self-consistent mean-field densities

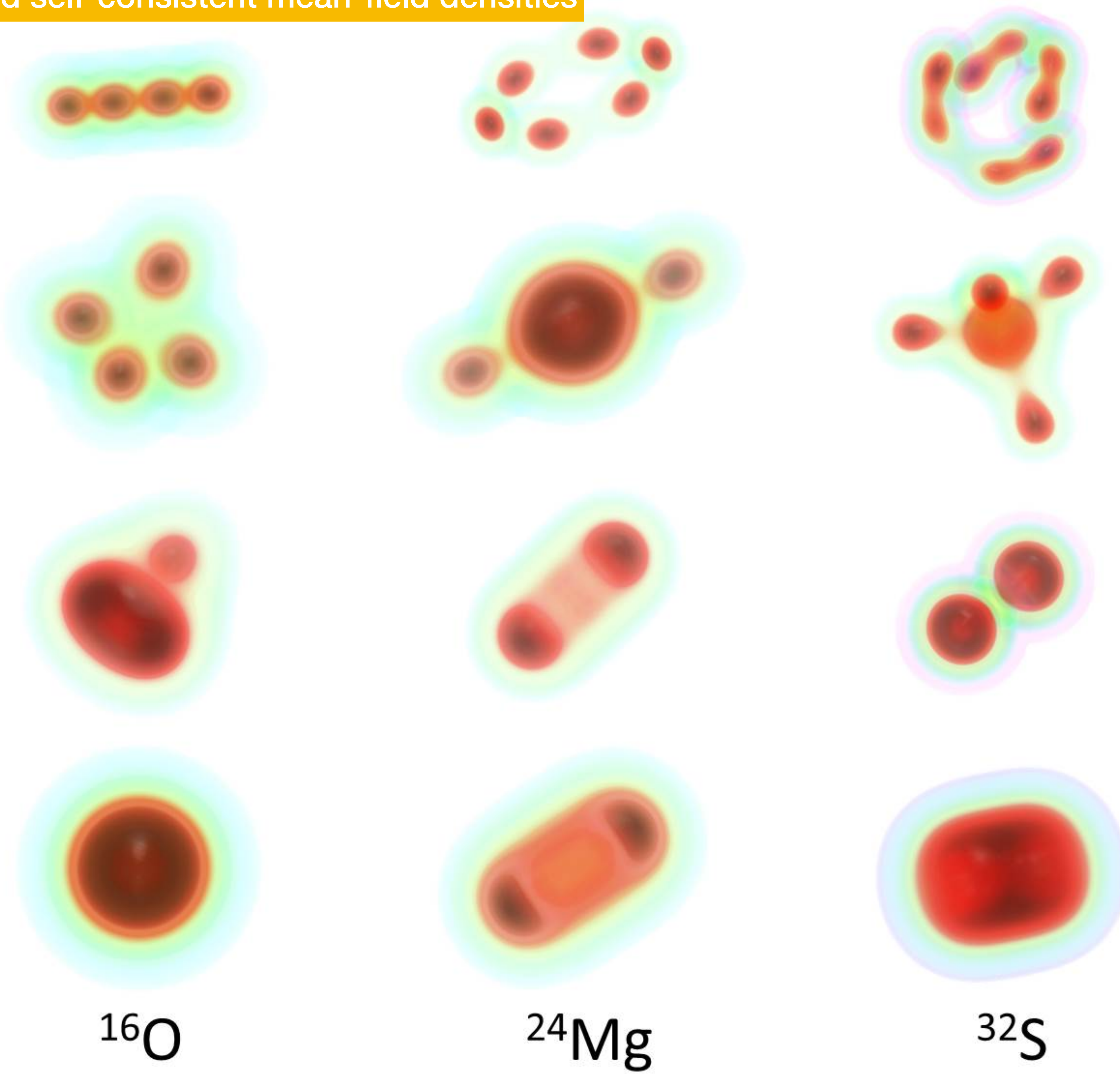

Beyond self-consistent mean field: collective correlations related to symmetry restoration and nuclear shape fluctuations

Quadrupole and octupole collectivity and cluster structures in neon isotopes

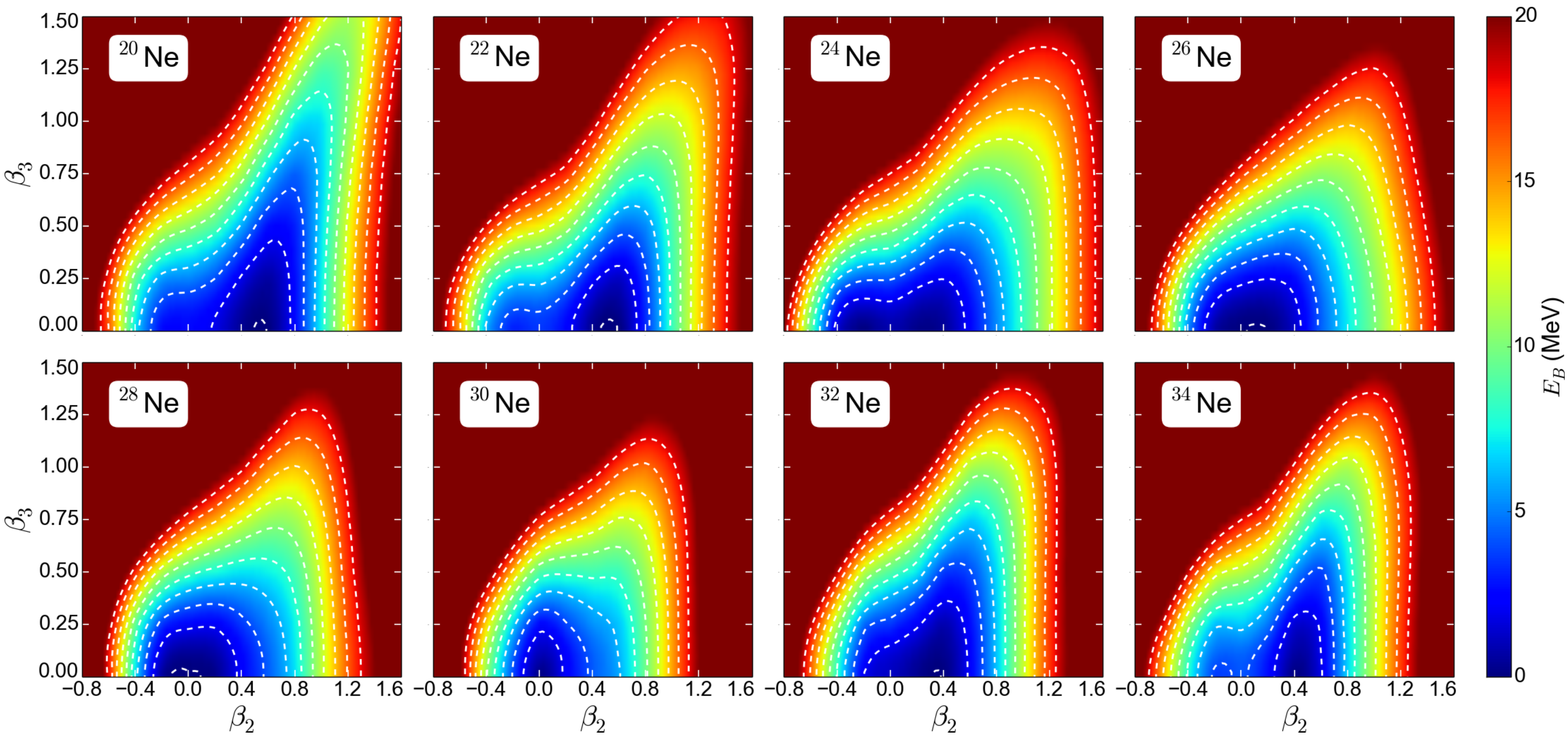

PHYSICAL REVIEW C **97**, 024334 (2018)

GCM configuration mixing of angular-momentum and parity projected SCMF states

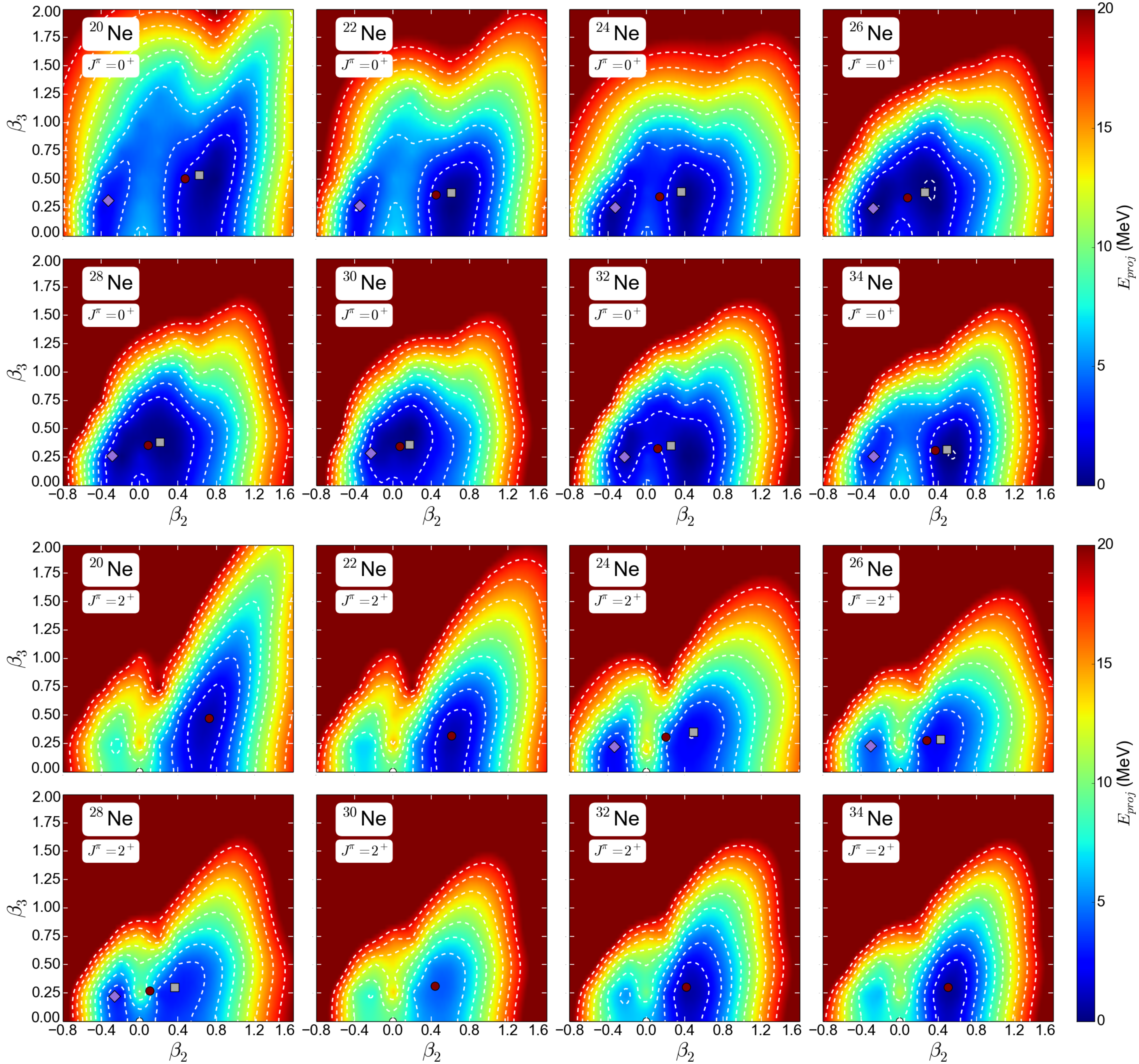

GCM configuration mixing of angular-momentum and parity projected SCMF states

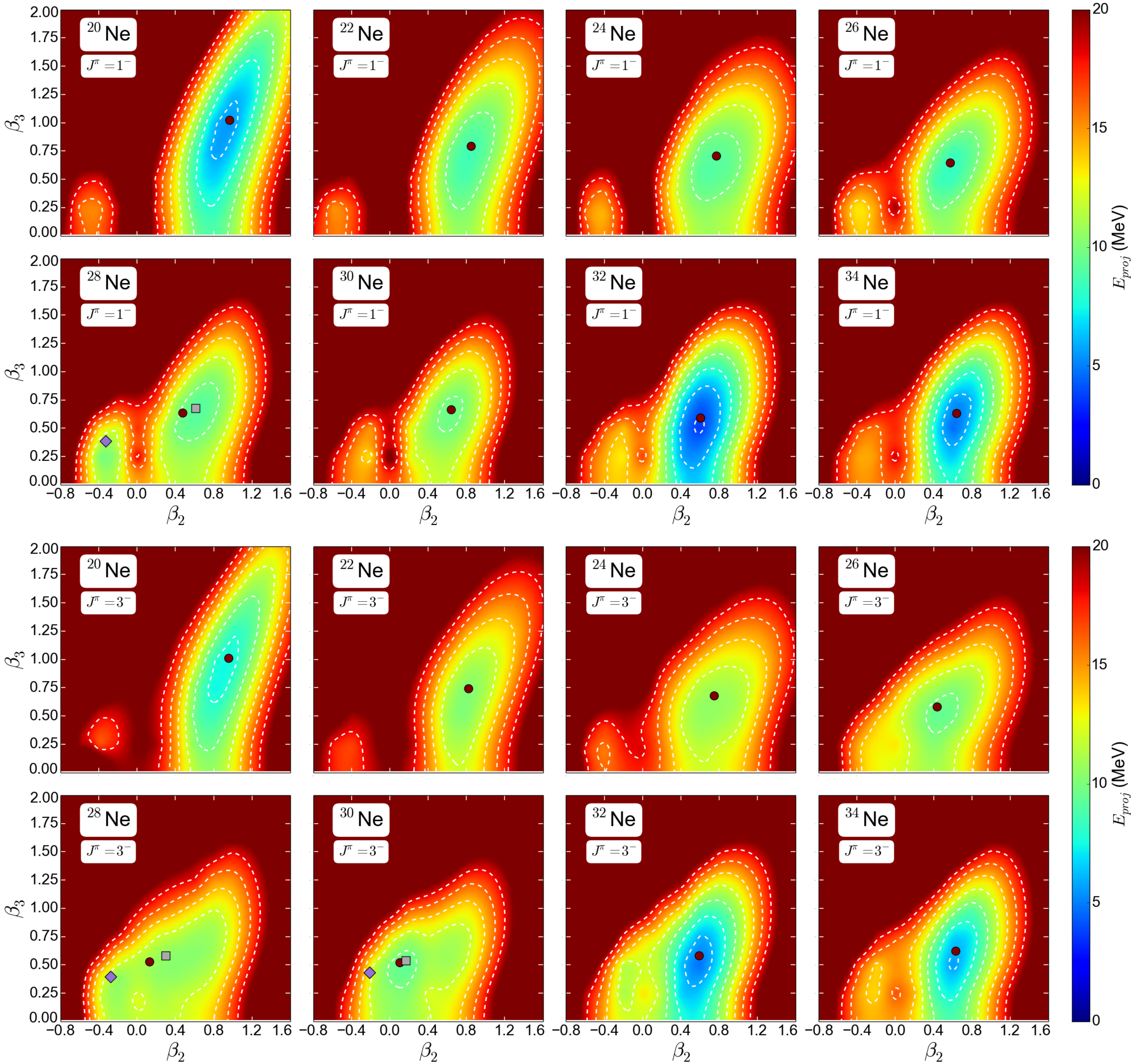

GCM configuration mixing of angular-momentum and parity projected SCMF states

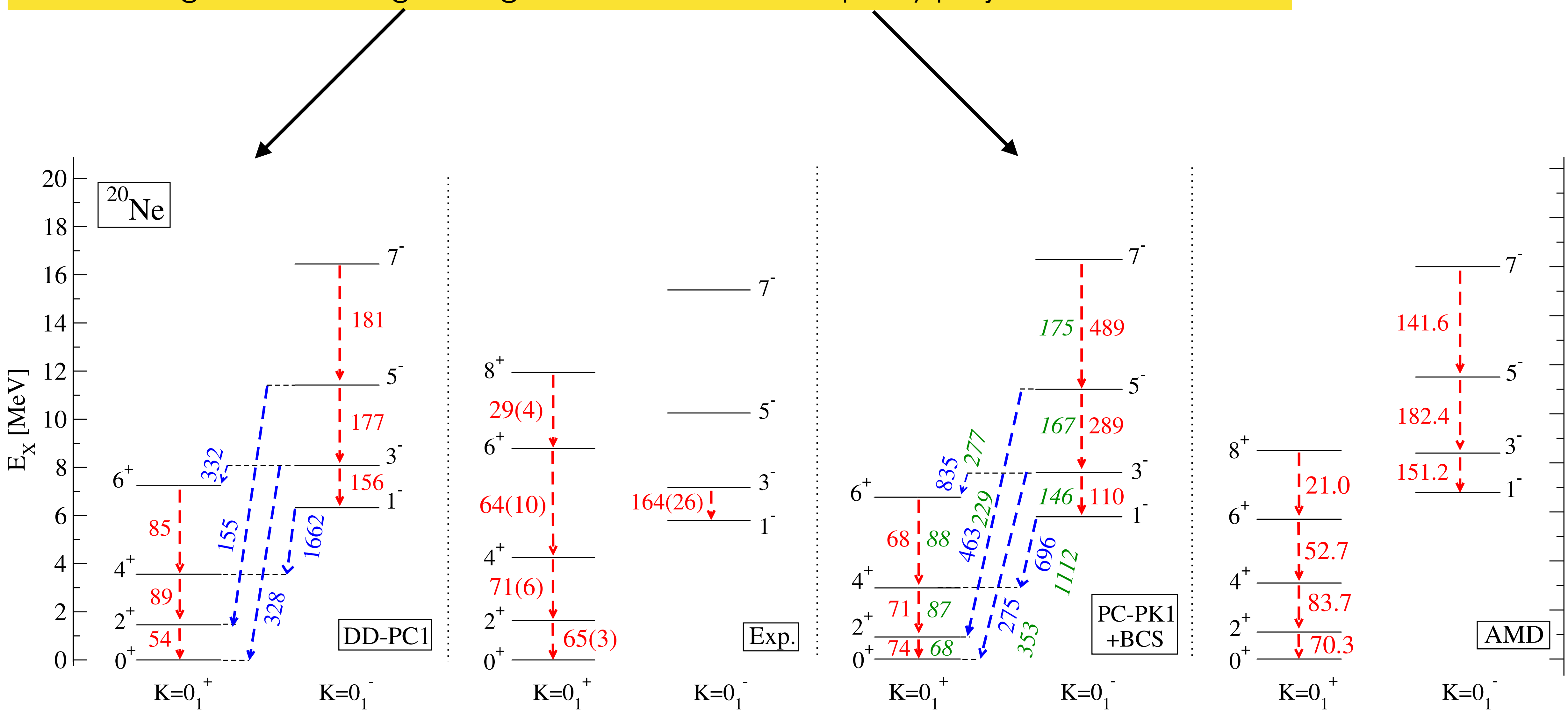

PHYSICAL REVIEW C **97**, 024334 (2018)

Amplitudes of GCM collective wave functions squared.

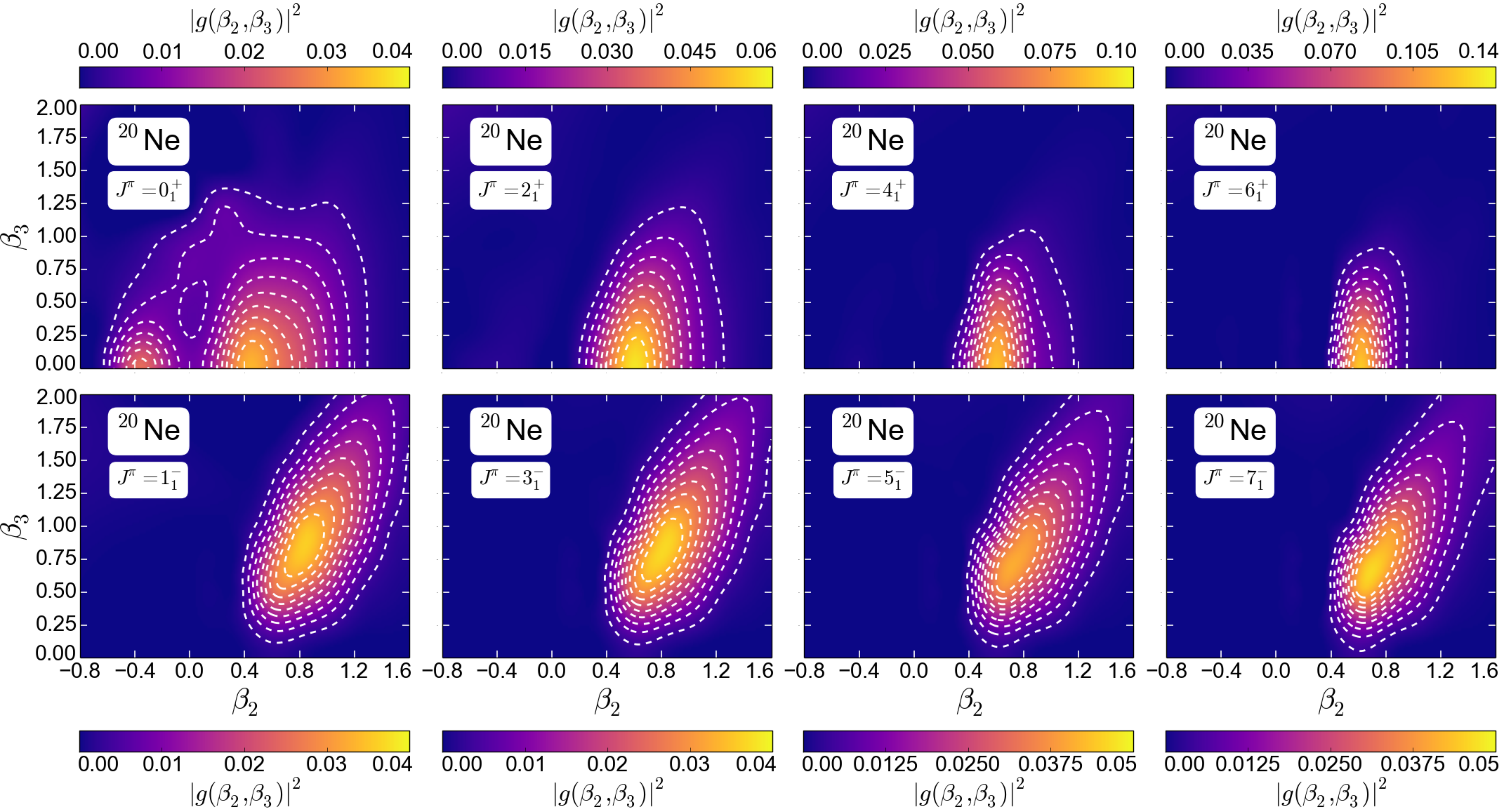

Expectation values of of the quadrupole and octupole deformation parameters in the correlated GCM states:

$$\langle \beta_\lambda \rangle_\alpha^{J\pi} = \sum_i |g_\alpha^{J\pi}(q_i)|^2 \beta_{\lambda i}$$

characteristic intrinsic densities at these deformations:

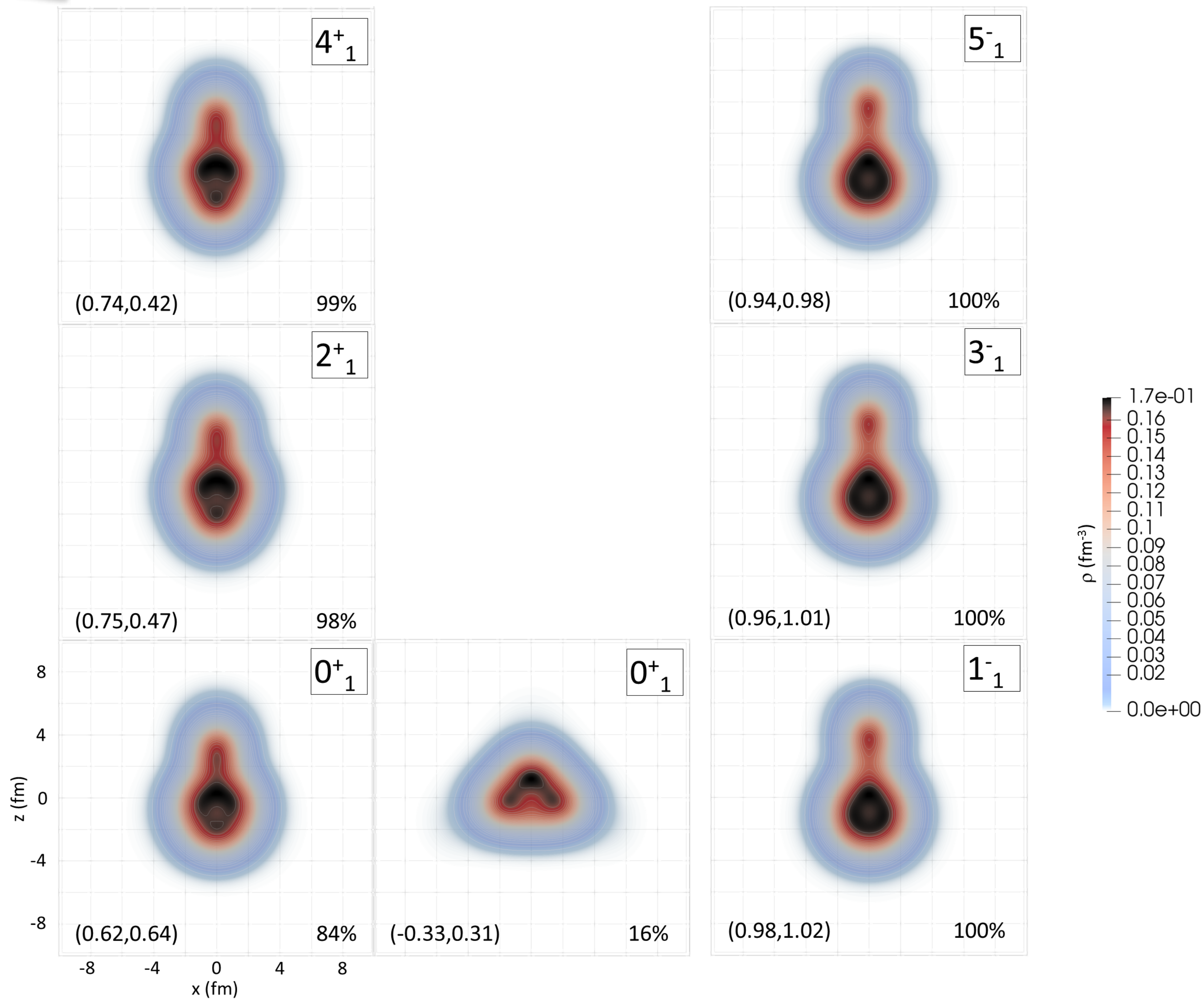

Neutron-rich Ne isotopes

PHYSICAL REVIEW C **97**, 024334 (2018)

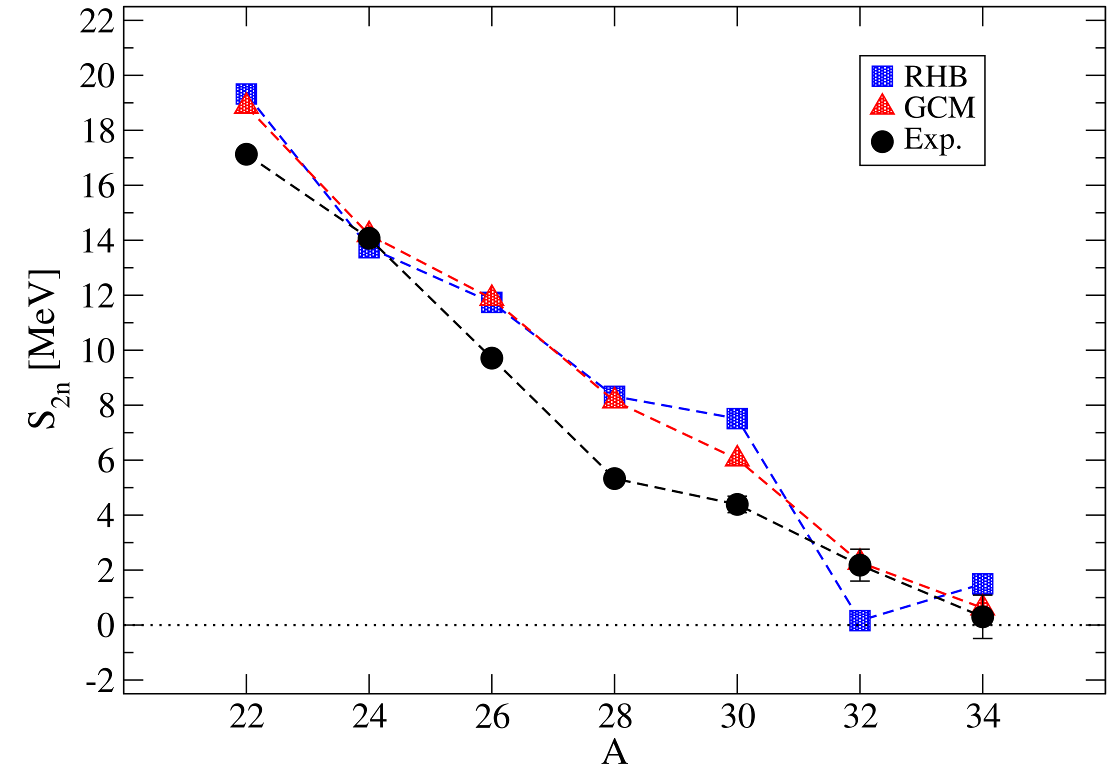

GCM spectra: DD-PC1 + separable pairing

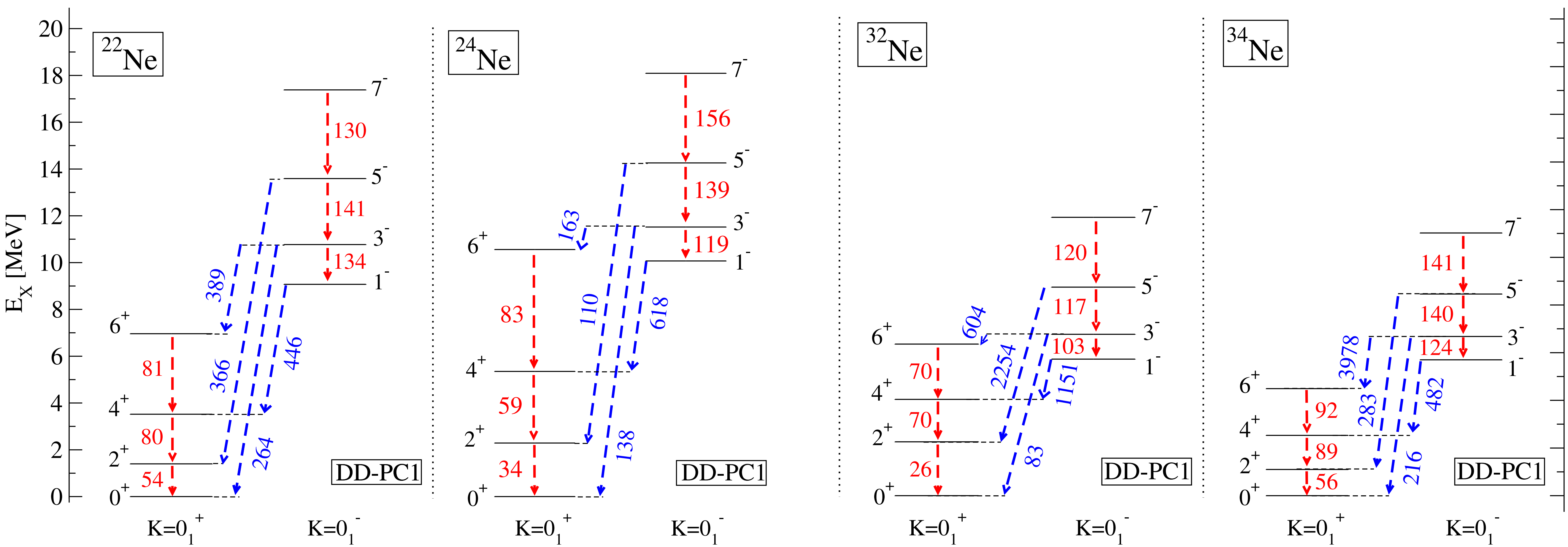

^{22}Ne - intrinsic densities at characteristic prolate (oblate) deformations:

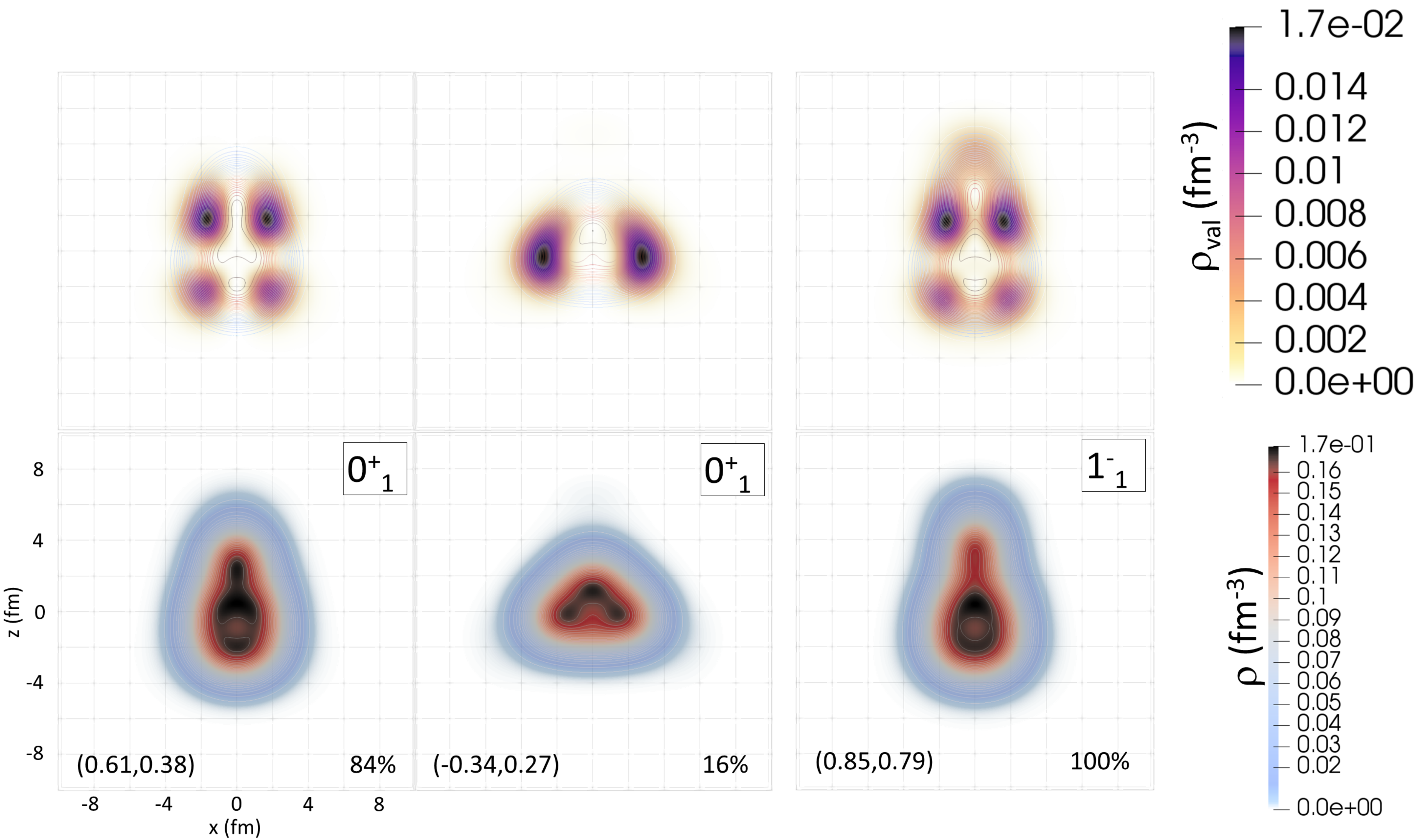

^{24}Ne - intrinsic densities at characteristic prolate (oblate) deformations:

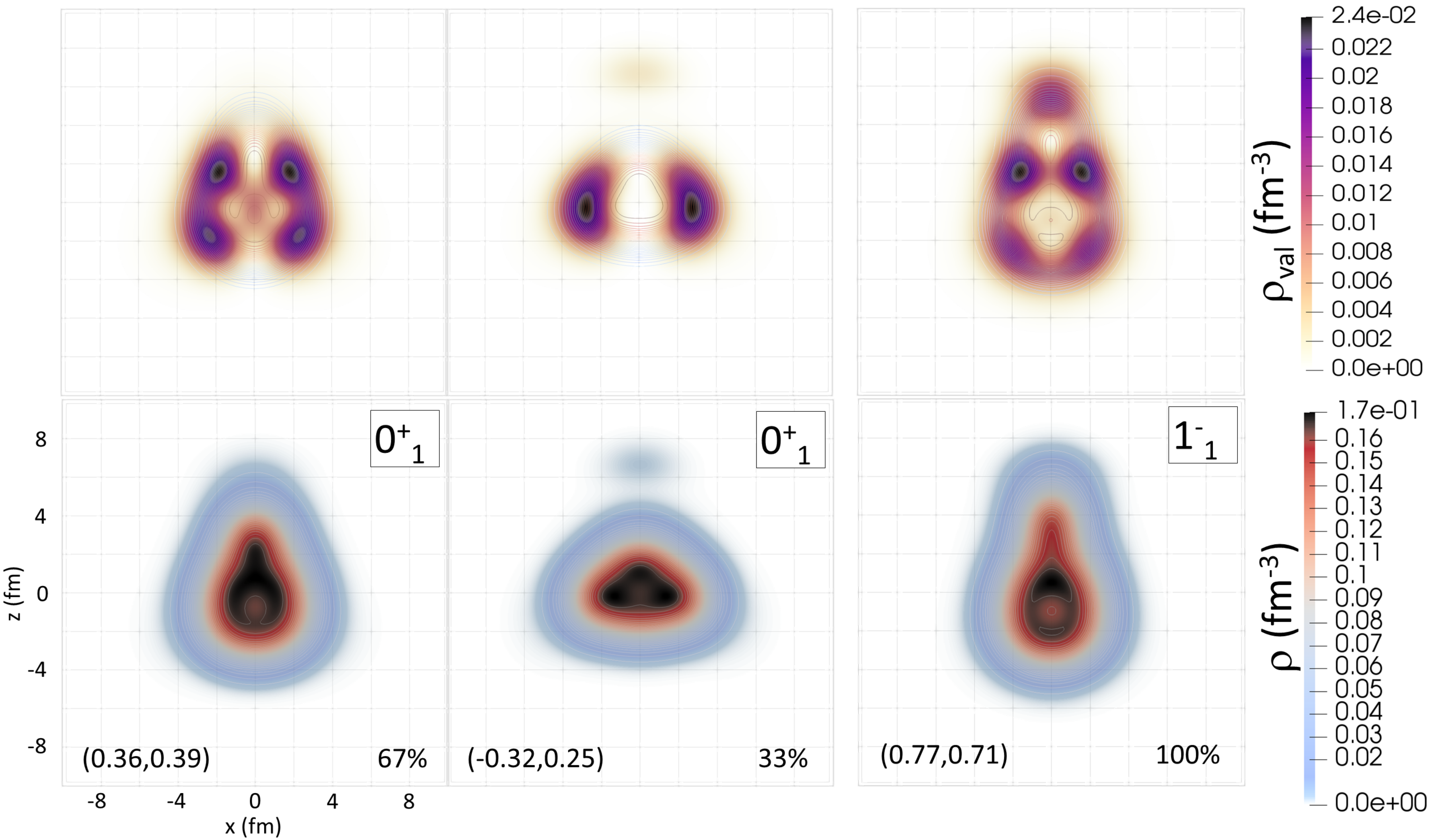

Cluster structures in ^{12}C

PHYSICAL REVIEW C **99**, 034317 (2019)

Energy density functional DD-PC1 + separable pairing interaction

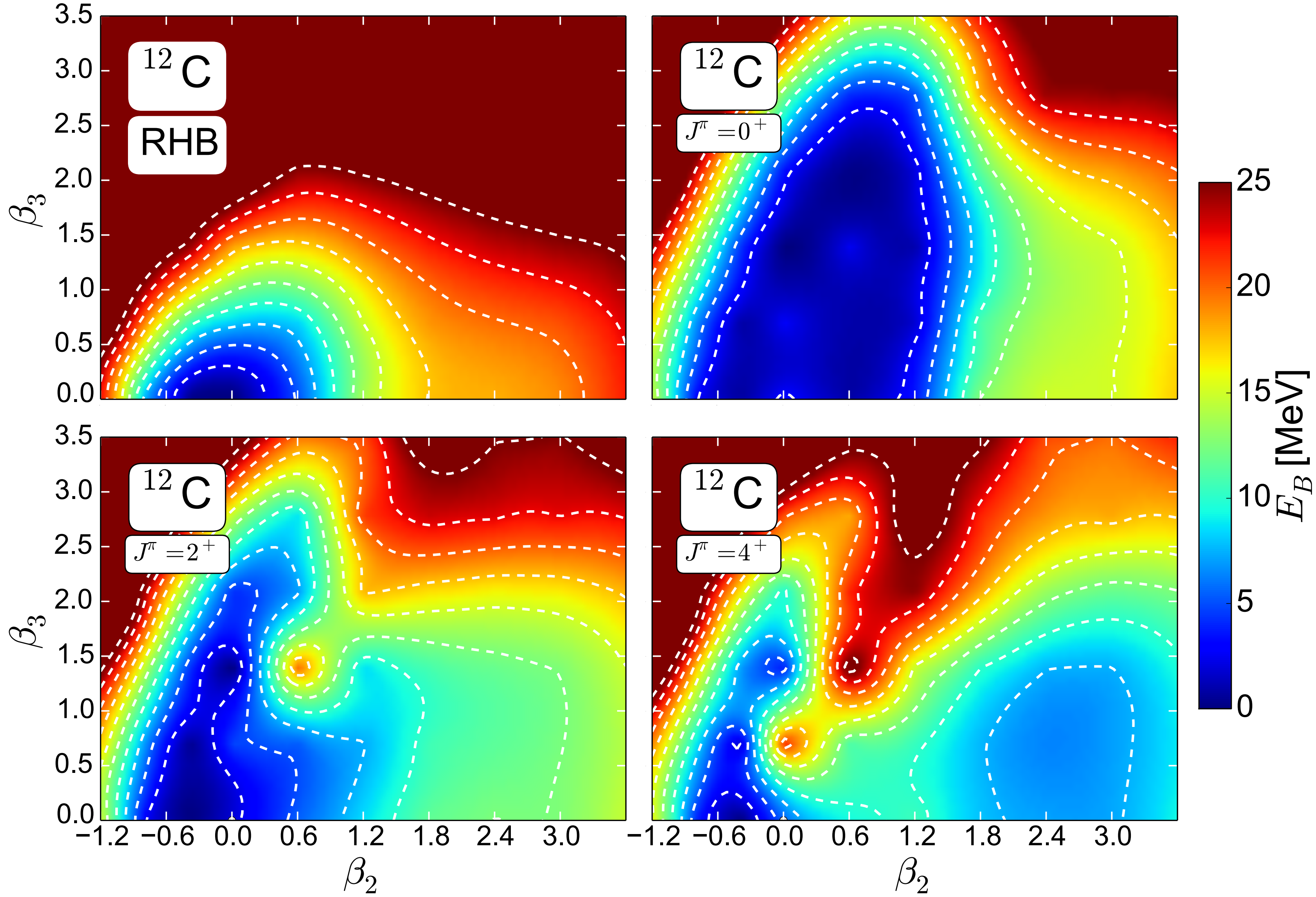

Deformation energy surfaces of ^{12}C in the β2-β3 plane: self-consistent mean-field RHB, angular momentum-, particle number-, and parity-projected for spin-parity values $J^{\pi} = 0^{+}, 2^{+}, 4^{+}$.

Spectroscopy of collective states

PHYSICAL REVIEW C **99**, 034317 (2019)

GCM configuration mixing of angular momentum-, particle number-, and parity-projected SCMF states:

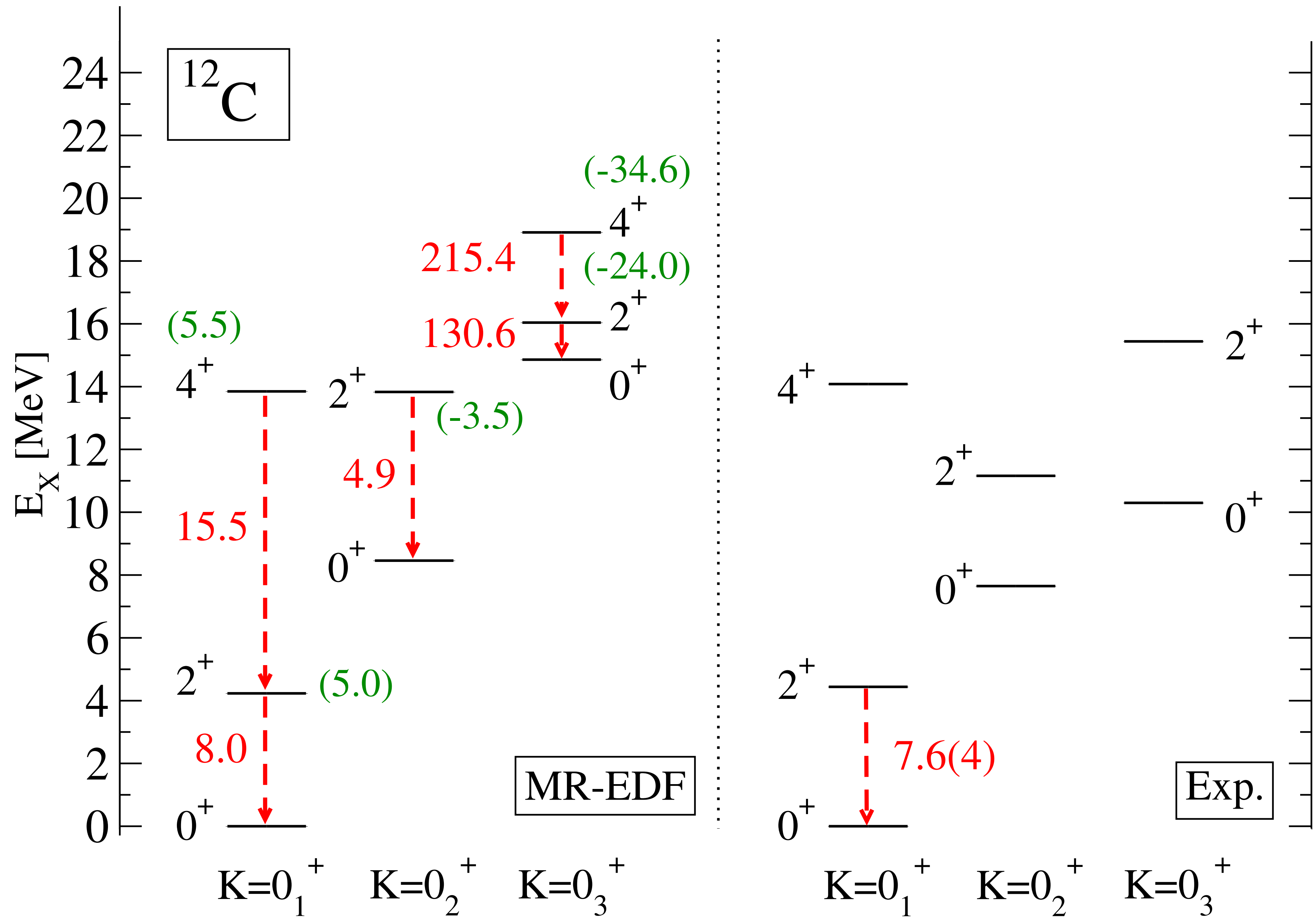

Amplitudes of collective wave functions squared $|g(\beta 2,\beta 3)|^2$ for the low-energy levels of ^{12}C.

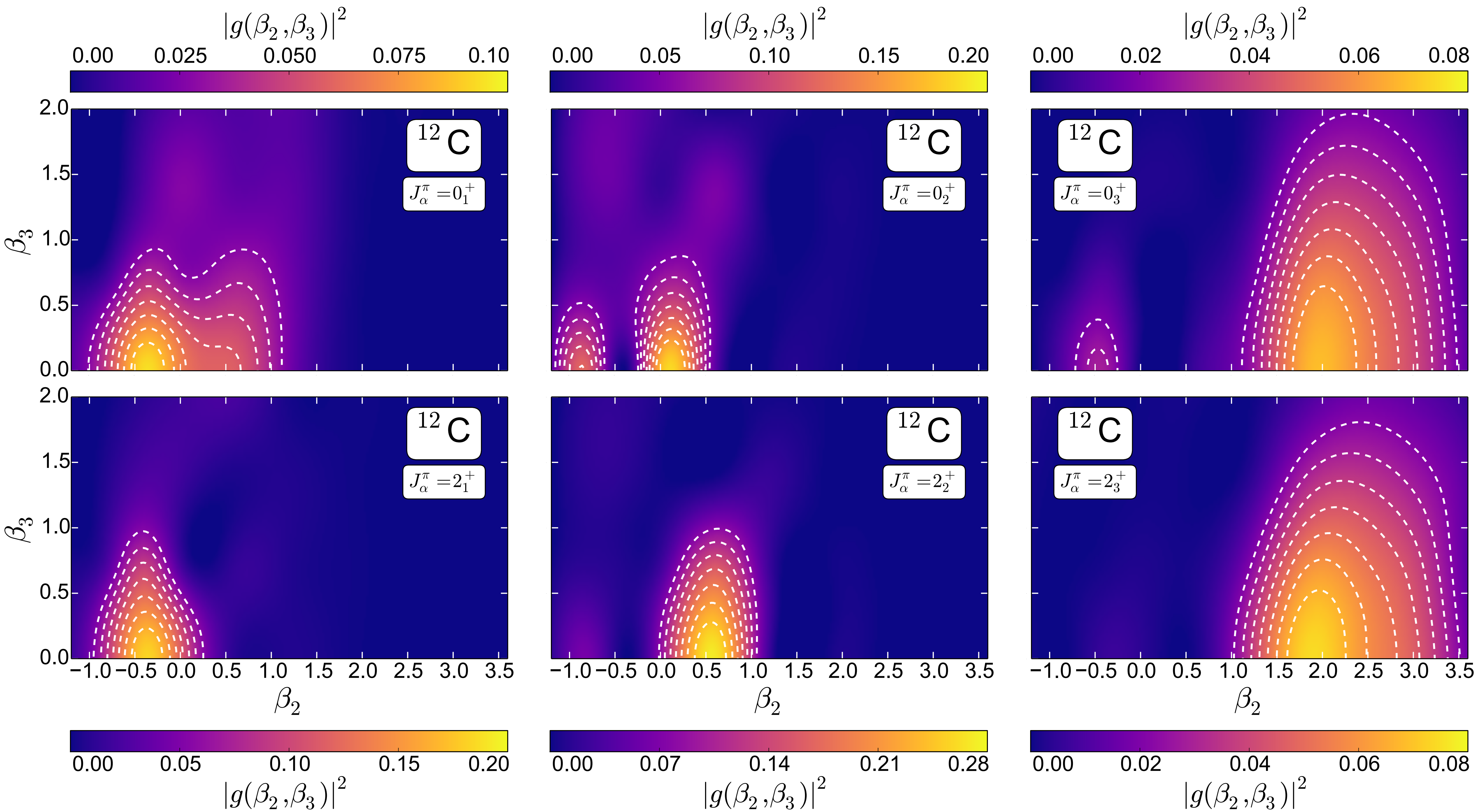

Collective states in the intrinsic frame

...calculate the expectation values of deformation parameters β2 and β3 for each collective state:

$$\langle \beta_2 \rangle_\alpha^{J;NZ;\pi} = \sum_i \left| g_\alpha^{J;NZ;\pi}(q_i) \right|^2 \beta_{2i},$$

$$\langle |\beta_3| \rangle_\alpha^{J;NZ;\pi} = \sum_i \left| g_\alpha^{J;NZ;\pi}(q_i) \right|^2 |\beta_{3i}|,$$

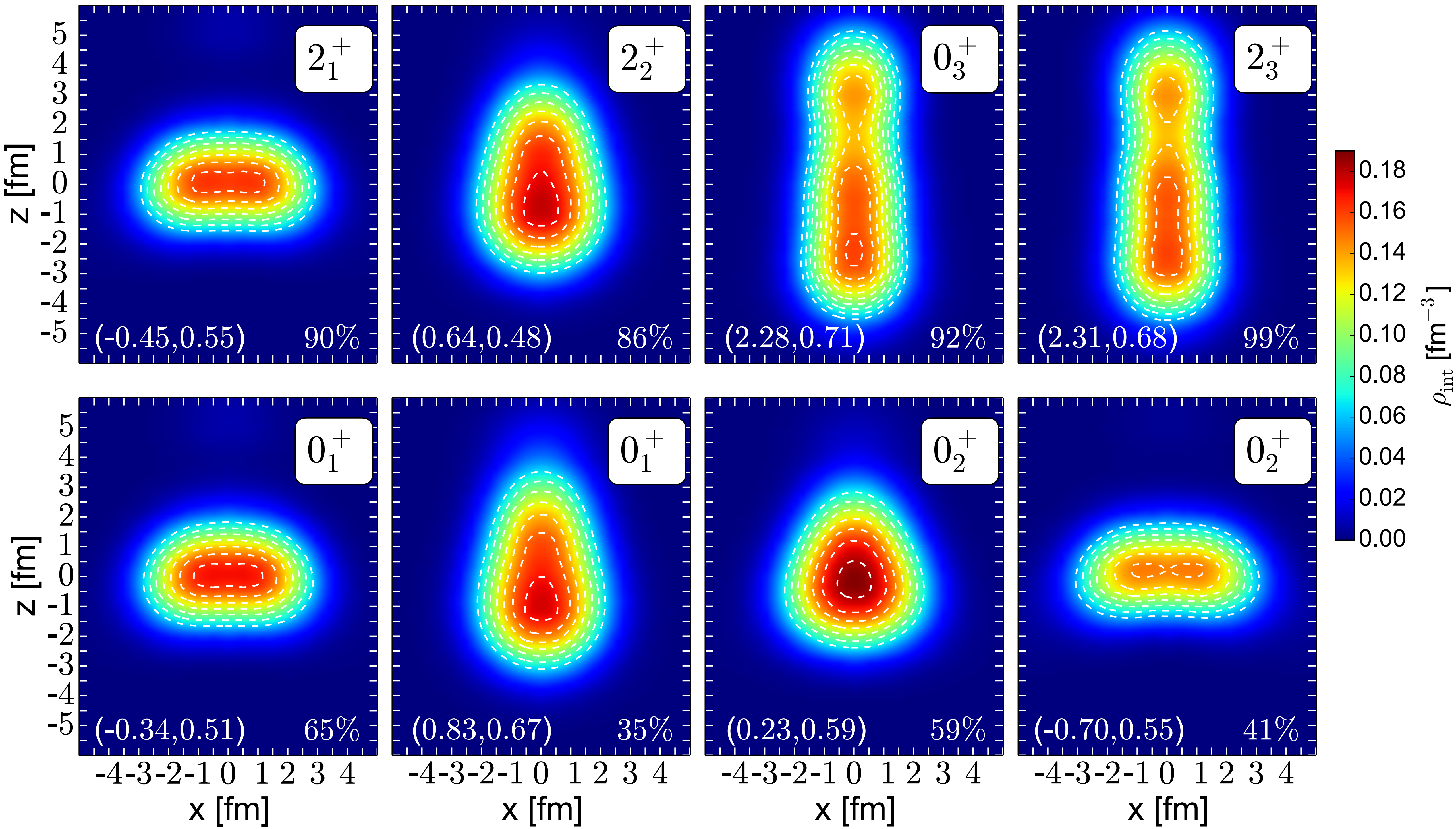

Electron-nucleus scattering form factors

…longitudinal Coulomb form factor:

$$F_L(q) = \frac{\sqrt{4\pi}}{Z}\int_0^\infty dr r^2 \rho^{J_f\alpha_f}_{J_i\alpha_i,L}(r) j_L(qr),$$

reduced proton transition density:

$$\rho^{J_f\alpha_f}_{J_i\alpha_i,L}(r) = (-1)^{J_f-J_i}\frac{2J_f+1}{2J_i+1}\sum_K \langle J_f 0 L K | J_i K\rangle \times \int d\hat{\mathbf{r}}\,\rho^{J_f J_i K 0}_{\alpha_f \alpha_i}(\mathbf{r}) Y^*_{LK}(\hat{\mathbf{r}}),$$

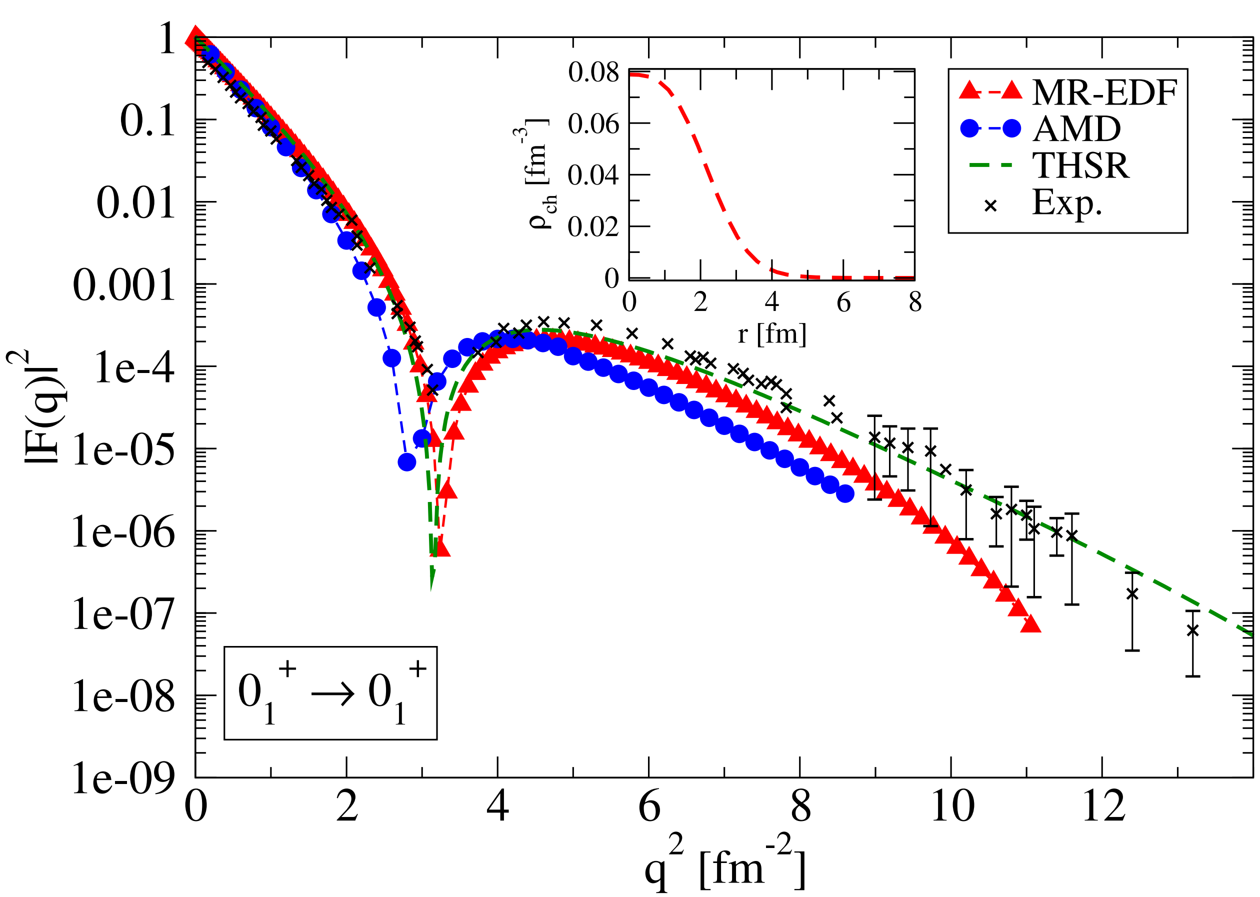

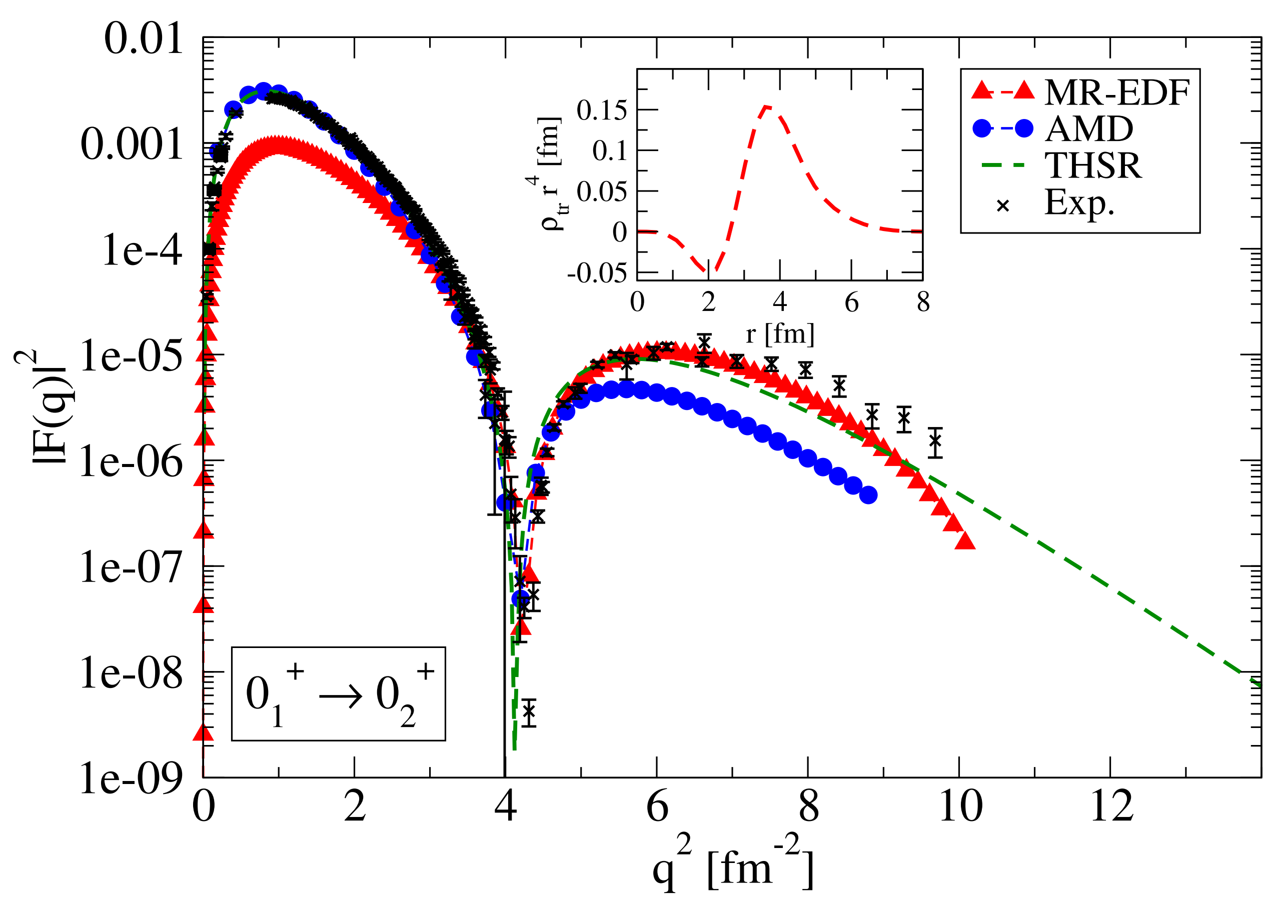

PHYSICAL REVIEW C **99**, 034317 (2019)

- P. Marević
- R.-D. Lasseri
- J.-P. Ebran
- E. Khan
- T. Nikšić
- D. Vretenar